

Suppression of driving laser in high harmonic generation with a microchannel plate

Qi Zhang, Kun Zhao, Jie Li, Michael Chini, Yan Cheng, Yi Wu, Eric Cunningham, and Zenghu Chang*

*Institute for the Frontier of Attosecond Science and Technology, CREOL and Department of Physics,
University of Central Florida, Orlando, Florida 32816, USA*

*Corresponding author: Zenghu.Chang@ucf.edu

Received February 7, 2014; revised May 14, 2014; accepted May 14, 2014;
posted May 15, 2014 (Doc. ID 206119); published June 13, 2014

Separating the infrared driving laser from the extreme ultraviolet (XUV) pulses after high-order harmonic generation has been a long-standing difficulty. In this Letter, we propose and demonstrate that the driving laser can be blocked by simply installing a microchannel plate (MCP) into the beam line. In addition to its high damage threshold, the MCP filter also transmits photons over the entire XUV region. This paves the way for attosecond pulse generation with unprecedented bandwidth. © 2014 Optical Society of America

OCIS codes: (020.2649) Strong field laser physics; (320.6629) Supercontinuum generation; (320.7100) Ultrafast measurements.

<http://dx.doi.org/10.1364/OL.39.003670>

Since the first experimental demonstration of attosecond pulses from high-order harmonic generation (HHG) in 2001 [1], the development of time-resolved spectroscopic techniques with attosecond temporal precision has greatly had an impact on our understanding of ultrafast electron dynamics in atomic, molecular, and condensed-matter systems [2–4]. When an intense few-cycle laser pulse—usually with a central wavelength in the near-infrared (NIR) or mid-infrared (MIR) region—is focused onto a gaseous target, high-order harmonics are generated as a coherent beam of extreme ultraviolet (XUV) light, which copropagates with the residual driving laser. The bandwidth of this new optical source can extend from the vacuum ultraviolet [5] to the x-ray spectral region [6] and allows the generation of isolated attosecond pulses with extremely short durations [7–10].

However, for many experimental applications, one must separate the generated XUV from the residual driving laser pulses to avoid ionization or excitation of the target by the strong laser field. This becomes a significant technical challenge, especially when high-energy (>100 mJ) driving pulses are used to generate high-flux XUV pulses [11] or when an MIR laser is used to extend the HHG cutoff [12,13]. To solve this issue, several schemes have been proposed and demonstrated: thin-film metallic filters [1–10], an annular pump beam [14], a dichroic beam splitter [15], a Si/SiC plate at the Brewster angle [16], and diffraction gratings [17]. However, each of those schemes has certain limitations.

The use of a thin metallic filter (hundreds of nanometers in thickness) is the most common way to block the driving beam, while transmitting the XUV. Although metal filters with transmission windows in the XUV region are available, they are limited to a finite range of photon energies, which ultimately limits the achievable attosecond pulse duration. Furthermore, in some cases no suitable filter can be found, such as for the study of molecular targets where photon energies ranging from <10 to 20 eV are desired [18]. Moreover, metallic filters are extremely fragile, and some filters such as zirconium (Zr) are susceptible to damage from high-energy driving lasers. While the use of an annular driving beam

eliminates the damage issue [14], a significant portion of the driving laser energy is lost, thus limiting the flux of the generated high-order harmonics.

Another technique involves the use of dichroic multilayer mirrors, which have high reflectivity in the XUV and low reflectivity for the NIR [15]. However, the coating design and the manufacturing process are rather complicated, and the high XUV reflectivity can only be obtained within a narrow wavelength range due to the lack of suitable coating materials. Alternatively, an Si/SiC plate placed at the Brewster angle of the driving laser wavelength has been demonstrated [16]. For the NIR driving laser, the Brewster angle is around 70° for Si/SiC, and ~50% reflectivity can be obtained for XUV photon energies up to 60 eV. The Si/SiC beam splitter has a high damage threshold and can effectively eliminate the residual NIR. However, for MIR driving lasers, the Brewster angle reduces to ~50° for Si/SiC, for which the reflectivity is less than 5% for photon energies above ~30 eV. Therefore, this method is not suitable for broadband HHG driven by MIR lasers.

The most recently proposed scheme is to use diffraction gratings as the beam separator [17]. The grating system can, in principle, be designed for any wavelength range, and the damage threshold is high due to the grazing incidence angle on the grating. However, besides the complicated design and the low throughput for the XUV, this design cannot be applied for broadband attosecond pulses due to the spatial and temporal chirp introduced by the gratings [17].

In this Letter, we propose and demonstrate a simple solution for this long-standing problem, which is to use a microchannel plate (MCP) as an optical filter. The MCP filter can effectively block either NIR or MIR driving laser and transmit photons over the entire XUV and x-ray spectral regions. Essentially, an MCP consists of millions of parallel glass capillaries (microscopic channels), which lead from one surface to the other. The diameter of each channel is several micrometers, which is comparable with the wavelength of NIR/MIR but much larger than that of the XUV or soft x-ray photons. Therefore, the driving pulse propagating

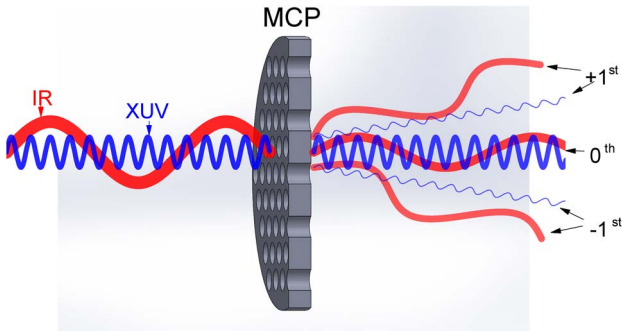


Fig. 1. Schematic of the principle of the MCP filter. The diameter of each MCP channel is comparable to the wavelength of the IR but much larger than that of the XUV. The red (blue) lines indicate the IR (XUV) beam. The 0th and ± 1 st order diffractions are labeled by black arrows.

through the MCP will be strongly diffracted, while the transmitted high harmonic beam is mainly unperturbed. Consequently, the MCP functions as a short-wavelength-pass filter between the driving NIR/MIR and XUV/x-ray photons. A schematic of the function of such a filter is shown in Fig. 1. This MCP filter is particularly desirable when a broad bandwidth of XUV photons is generated by an intense MIR pump laser.

In the experiments, the MCP (TecTra GmbH, MCP-25-40-d) has a channel diameter of $8\ \mu\text{m}$ and a thickness-to-diameter ratio of 40:1. The open area is 58%–60% of the total area, limiting the maximum value of the transmission. The bias angle, which must be carefully aligned along the laser propagation direction, is 8 deg. In order to demonstrate this new technique, the transmission of the MCP was measured as a function of wavelength for MIR, NIR, and visible laser sources as well as for XUV light from HHG.

The diffraction pattern of an NIR driving laser propagating through the MCP filter is shown in Fig. 2. The bright center spot is the zeroth-order transmission and follows the same path as the incident beam. All the non-zero-order diffraction beams can be blocked by an aperture placed after the MCP. Three lasers with different

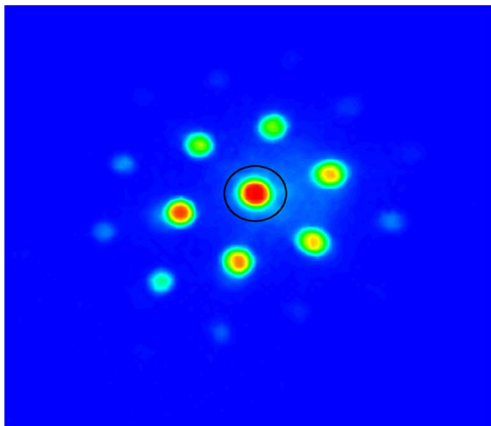


Fig. 2. Diffraction pattern after a Ti:Sapphire laser propagates through the MCP. The center bright spot circled by the black line is the zeroth-order transmission, which follows the same path as the incident beam. Higher diffraction orders are spatially separated, so they can be easily blocked.

wavelengths were available for testing the MCP transmission. The home-built Ti:Sapphire laser has a central wavelength of 750 nm and pulse duration of 23 fs. This type of laser is commonly used as the driving laser for HHG. The MIR output from a commercial TOPAS (Coherent, HE-TOPAS-Prime) has a central wavelength of $1.6\ \mu\text{m}$ and pulse duration of 50 fs. The continuous-wave laser with a wavelength at 532 nm (Opto Engine LLC, MLL-III-532 nm) was also used. The measured zeroth-order transmissions at these three different wavelengths are 0.4% for $1.6\ \mu\text{m}$, 5% for 750 nm, and 11% for 532 nm, respectively. It can be seen that the zeroth-order transmission largely depends on the wavelength of the incident beam.

The MCP transmission in the XUV spectral region has been measured in [19] to be as high as 60% for photon energies from 50 eV to 1.5 keV, reaching the upper limit set by the MCP opening ratio. It is reasonable to assume that the transmission should be the same for even higher energy photons due to their decreasing wavelengths. The measurement in [19] was done by placing an XUV photodiode 1 mm away from the MCP, indicating that the total transmission was measured. However, only the zeroth-order transmission is useful for studying ultrafast dynamics. Therefore, we evaluated the zeroth-order transmission of the MCP filter in the XUV by placing the filter in our HHG beam line [10]. A schematic drawing of the MCP filter in the experimental setup is shown in Fig. 3(a). Briefly, the high harmonics, generated in a neon gas target from 7 fs, 0.5 mJ laser pulses, passed through the MCP filter and were focused by a toroidal mirror to a second neon gas target for measurement of the photoelectron spectrum. The diffracted light was blocked using an aperture placed after the toroidal mirror, transmitting only the zeroth-order transmission.

The photoelectron spectrum of HHG with the MCP filter was recorded by a magnetic bottle electron spectrometer, as shown in Fig. 3(b). Photoelectron spectra taken with 300 nm aluminum (Al) and 300 nm zirconium (Zr) filters were also plotted in the same figure with their relative intensities adjusted for best comparison. The result shows that an HHG spectrum up to 150 eV photoelectron energy can be observed with the MCP filter, which agrees well with the spectra taken with Al and Zr filters.

The zeroth-order transmission of XUV through the MCP can be measured by comparing the photoelectron spectra with and without the MCP filter, as plotted in Fig. 4. The blue circles represent the transmission taken with the Al filter, and the red squares show the result with the Zr filter. This measurement shows that the zeroth-order transmission is about 25% for photon energies between 30 and 120 eV. There is a clear tendency that the transmission is larger for higher photon energy, suggesting the applicability of the MCP filter for high-photon energy and ultrabroadband attosecond pulse generation driven by MIR lasers.

The energy of the driving laser after passing through the MCP is less than $1\ \mu\text{J}$ and does not noticeably affect the photoelectron spectrum, allowing characterization of attosecond pulses with reconstruction of attosecond beating by interference of two-photon transitions (RABBITT) or phase retrieval by omega oscillation filtering (PROOF) [20,21]. Experimentally, the RABBITT

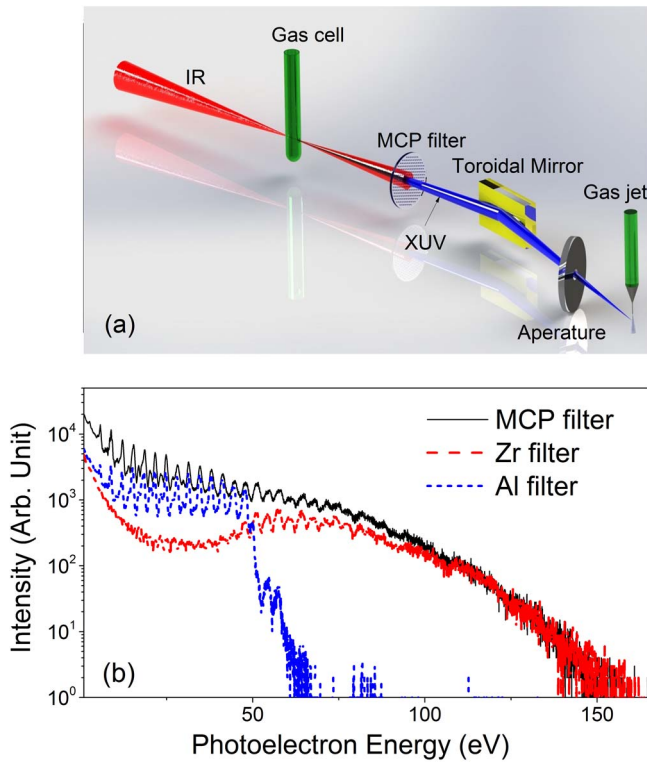


Fig. 3. (a) Schematic drawing of MCP filter in the HHG beam line to suppress the IR driving laser and transmit the XUV. The focused XUV photoionizes the neutral gas atoms (neon) from the gas jet, and the photoelectron spectra are recorded by a time-of-flight spectrometer (not shown). (b) Measured photoelectron spectra with MCP (black solid), Zr (red dash), and Al filters (blue dot). The relative intensities of the spectra are adjusted for best comparison.

spectrograms were recorded with and without the MCP filter as shown in Fig. 5(a). The details of the setup can be found in [10]. A 300 nm Al foil was used in both cases to block the driving IR when no MCP filter was present. The black-dashed lines were plotted to indicate the trend of the sideband peak positions. To quantitatively compare

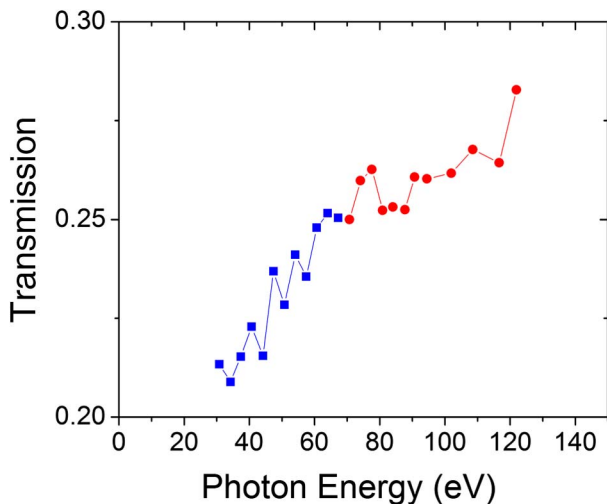


Fig. 4. Zeroth-order transmission of the XUV through an 8 μm pore MCP derived from measurements with Al (blue square) and Zr (red circle) filters.

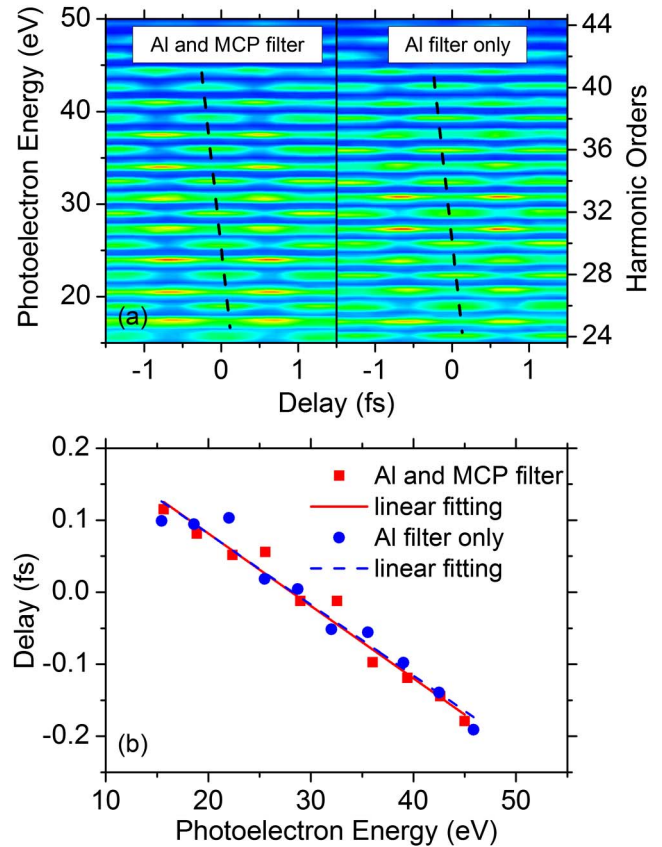


Fig. 5. (a) RABBITT spectrograms with (left) and without (right) MCP filter. (b) Relative delay for sideband maxima as the function of the photoelectron energy. Red squares were taken with Al and MCP filter; blue dots were taken with Al filter only. The linear fits for each dataset were plotted in the solid and dashed lines with the same color.

the RABBITT spectrograms with and without the MCP filter, we plot the delay for each sideband maximum as a function of the photoelectron energy in Fig. 5(b). The dots (red: MCP + Al; blue: Al only) are the experimentally measured delays corresponding to the sideband maxima, while the solid lines are linear fits to the data. It can be seen that the two lines overlap very well, demonstrating that the MCP has a negligible effect on the harmonic spectral phase. Further calculation is necessary to fully understand the XUV propagation within the MCP filters [22].

The damage threshold of the MCP filter was measured to be approximately 16 mJ/cm^2 using a 10 Hz, 800 nm Ti-Sapphire laser with about 25 fs duration, corresponding to an intensity of $0.6 \times 10^{12} \text{ W}/\text{cm}^2$. This value is comparable with the damage threshold of Si/SiC beam splitters reported in [16] and to our measured damage threshold of a 650 nm Al foil.

In conclusion, we have demonstrated that an MCP can be used as an effective beam separator in high-order harmonic and attosecond pulse generation based on the wavelength-dependent transmission. The zeroth-order transmission for various wavelengths was measured, and a transmission of about 25% was observed for XUV between photon energy of 30 and 120 eV. There is no additional spectral dispersion introduced by the MCP, and the filter can be applied to attosecond measurements, as

verified by RABBITT spectrograms taken with and without the MCP filter. In the future, an MCP with a larger open-area ratio and smaller pore size should be used to increase the zeroth-order transmission for the XUV and to decrease that of the driving laser. Compared with other techniques, this method is easy to implement, and the MCP filter transmits photons over the entire XUV and x-ray spectrum. Moreover, it is an effective method for blocking MIR laser sources, which may be used to generate even shorter attosecond pulses with broader bandwidths.

More generally, we wish to emphasize that the MCP here functions as a short-wavelength-pass filter to separate radiation of two wavelengths, which do not have to be NIR/MIR and XUV/soft x ray. Also, since the suppression of the long wavelength is not realized by a coating on a substrate-like some optical filters, there is no dispersion or absorption of the transmitting wavelength by either the coating or the substrate. This is extremely critical in ultrashort optical pulse generation and its applications. Therefore, an MCP can be a useful short-wavelength-pass filter in a broad range of ultrafast studies.

We appreciate the help of H. Hua, D. Hagan, and E. Van Stryland for the use of the TOPAS laser. The work is funded by the National Science Foundation under grant no. 1068604, the Army Research Office, and the DARPA PULSE program by a grant from AMRDEC.

References

1. M. Hentschel, R. Kienberger, Ch. Spielmann, G. A. Reider, N. Milosevic, T. Brabec, P. Corkum, U. Heinzmann, M. Drescher, and F. Krausz, *Nature* **414**, 509 (2001).
2. J. Itatani, J. Levesque, D. Zeidler, H. Niikura, H. Pépin, J. C. Kieffer, P. B. Corkum, and D. M. Villeneuve, *Nature* **432**, 867 (2004).
3. R. Kienberger, E. Goulielmakis, M. Uiberacker, A. Baltuška, V. Yakovlev, F. Bammer, A. Scrinzi, Th. Westerwalbesloh, U. Kleineberg, U. Heinzmann, M. Drescher, and F. Krausz, *Nature* **427**, 817 (2004).
4. A. L. Cavalieri, N. Müller, Th. Uphues, V. S. Yakovlev, A. Baltuška, B. Horvath, B. Schmidt, L. Blümel, R. Holzwarth, S. Hendel, M. Drescher, U. Kleineberg, P. M. Echenique, R. Kienberger, F. Krausz, and U. Heinzmann, *Nature* **449**, 1029 (2007).
5. D. C. Yost, T. R. Schibli, J. Ye, J. L. Tate, J. Hostetter, M. B. Gaarde, and K. J. Schafer, *Nat. Phys.* **5**, 815 (2009).
6. J. Seres, E. Seres, A. J. Verhoef, G. Tempea, C. Strelti, P. Wobrauschek, V. Yakovlev, A. Scrinzi, C. Spielmann, and F. Krausz, *Nature* **433**, 596 (2005).
7. M. Chini, K. Zhao, and Z. Chang, *Nat. Photonics* **8**, 178 (2014).
8. E. Goulielmakis, M. Schultze, M. Hofstetter, V. S. Yakovlev, J. Gagnon, M. Uiberacker, A. L. Aquila, E. M. Gullikson, D. T. Attwood, R. Kienberger, F. Krausz, and U. Kleineberg, *Science* **320**, 1614 (2008).
9. G. Sansone, E. Benedetti, F. Calegari, C. Vozzi, L. Avaldi, R. Flammini, L. Poletto, P. Villoresi, C. Altucci, R. Velotta, S. Stagira, S. De Silvestri, and M. Nisoli, *Science* **314**, 443 (2006).
10. K. Zhao, Q. Zhang, M. Chini, Y. Wu, X. Wang, and Z. Chang, *Opt. Lett.* **37**, 3891 (2012).
11. Y. Wu, E. Cunningham, J. Li, H. Zang, M. Chini, X. Wang, Y. Wang, K. Zhao, and Z. Chang, *Appl. Phys. Lett.* **102**, 201104 (2013).
12. B. Shan and Z. Chang, *Phys. Rev. A* **65**, 011804(R) (2001).
13. T. Popmintchev, M. Chen, D. Popmintchev, P. Arpin, S. Brown, S. Ališauskas, G. Andriukaitis, T. Balčiunas, O. D. Mücke, A. Pugzlys, A. Baltuška, B. Shim, S. E. Schrauth, A. Gaeta, C. Hernández-García, L. Plaja, A. Becker, A. Jaron-Becker, M. M. Murnane, and H. C. Kapteyn, *Science* **336**, 1287 (2012).
14. J. Peatross, J. L. Chaloupka, and D. D. Meyerhofer, *Opt. Lett.* **19**, 942 (1994).
15. R. W. Falcone and J. Bokor, *Opt. Lett.* **8**, 21 (1983).
16. E. J. Takahashi, H. Hasegawa, Y. Nabekawa, and K. Midorikawa, *Opt. Lett.* **29**, 507 (2004).
17. F. Frassetto, P. Villoresi, and L. Poletto, *J. Opt. Soc. Am. A* **25**, 1104 (2008).
18. G. Sansone, M. Reduzzi, A. Dubrouil, C. Feng, M. Nisoli, F. Calegari, C. Lin, W. Chu, L. Poletto, and F. Frassetto, in *Conference on Lasers and Electro-Optics*, OSA Technical Digest (online) (Optical Society of America, 2013), paper QF2C.1.
19. Z. Cao, F. Jin, J. Dong, Z. Yang, X. Zhan, Z. Yuan, H. Zhang, S. Jiang, and Y. Ding, *Opt. Lett.* **38**, 1509 (2013).
20. H. G. Muller, *Appl. Phys. B* **74**, S17 (2002).
21. M. Chini, S. Gilbertson, S. D. Khan, and Z. Chang, *Opt. Express* **18**, 13006 (2010).
22. S. V. Kulklevsky, F. Flora, A. Marinai, K. Negrea, L. Palladino, A. Reale, G. Tomassetti, A. Ritucci, G. Nyitray, and L. Kozma, *Appl. Opt.* **39**, 1059 (2000).